Density Functional Investigation of Thioepoxidated and Thiolated Graphene

ARTICLE *in* THE JOURNAL OF PHYSICAL CHEMISTRY C · APRIL 2009

Impact Factor: 4.77 · DOI: 10.1021/jp808599w

1 AUTHOR:

Pablo A. Denis
University of the Republic, Uruguay
104 PUBLICATIONS **1,526** CITATIONS

Article

Density Functional Investigation of Thioepoxidated and Thiolated Graphene

Pablo A. Denis

J. Phys. Chem. C, **2009**, 113 (14), 5612-5619• DOI: 10.1021/jp808599w • Publication Date (Web): 18 March 2009

Density Functional Investigation of Thioepoxidated and Thiolated Graphene

Pablo A. Denis†

Computational Nanotechnology, DETEMA, Facultad de Química, UDELAR, CC 1157, 11800 Montevideo, Uruguay

Received: September 29, 2008; Revised Manuscript Received: January 7, 2009

Employing first-principle calculations, we have investigated the interaction between graphene and the thioepoxide and thiol groups. The SH radical cannot be chemisorbed on perfect graphene, although it is physisorbed. The chemisorption energy can be increased to 0.4 eV if multiple SH groups are bonded to the sheet or if they are attached to Stones−Wales defects. However, when free-energy corrections are considered, the addition of SH groups to perfect graphene is not spontaneous. In the case of the SW defects, the addition is favorable if two SH groups are attached to the shortest CC bond and in opposite sites of the sheet. The single vacancy defect site has the highest affinity for the SH radical, which is dissociatively attached. Finally, employing nanoribbons, we have simulated the reactivity of bare and hydrogen-terminated edges of graphene. The SH group is dissociatively bonded to bare edges. However, hydrogen-terminated zigzag edges prefer to bind the SH group. Considering the different reactivities observed, the defect sites and edges of graphene can be labeled by employing SH radicals. The sites containing sulfur can be used to attach gold nanoparticles or create vertical arrays of graphene sheets on Au surfaces. Finally, for thioepoxidated graphene, we have determined that the binding energy per S atom is 0.49 eV, larger than that determined for the thiol group but very small to be achieved experimentally because the free-energy change is expected to be close to 0 for this process. These results confirm the experimental evidence, which indicated that the sulfur-containing groups present in sulfur−graphite nanocomposites are attached to the edges of graphite, although vacancy defect sites must be considered. The electronic properties of the functionalized and defective graphene sheets are discussed. As a byproduct, we have found that the free-energy term may turn the attachment of a single HO group to graphene to be not spontaneous. Thus, the OH groups observed in graphene oxide are present at defect sites or agglomerated, to have their binding energy increased due to cooperative effects, confirming earlier experimental results.

1. Introduction

Since their discovery, carbon nanotubes (CNTs) were supposed to be the motor of the present nanotechnological revolution.[1] However, it is extremely difficult to produce CNTs with uniform diameter, length, and chirality in large quantities.[2−4] In addition, there is another huge problem; the CNTs present a large amount of structural defects that change their electronic properties.[5−8] For these reasons, a tremendous effort has been devoted to synthesize new carbon materials with uniform properties.[9,10] The breakthrough came in 2004 when Novoselov et al.[11,12] produced graphene by micromechanical cleavage of graphite. Graphene[11,12] and graphene oxide[13,14] are promising candidates to replace CNTs in a variety of technological applications because they have outstanding mechanical,[15,16] thermal,[17,18] spintronic−electronic,[19−21] drug delivery,[22] and catalytic[23] properties that can be used in many technological applications such us the detection of harmful species.[24,25] Therefore, a large number of investigations have been performed on graphene and graphite oxide,[11−25] but little is known about the interaction between sulfur and graphene sheets and also with graphite. This is somewhat surprising if we consider that graphite−sulfur composites present superconductive properties[26,27] and also that sulfur has been used to covalently immobilize biological molecules on CNTs.[28] This lack of information can be due, in part, to the fact that the interaction between sulfur and carbon nanotubes has been controversial.[29,30] However, Kurmaev et al.[26] and Da Silva et al.[27] showed that sulfur can be incorporated in large amounts into graphite at 5 and 23 wt % by a simple procedure. The X-ray analysis revealed a small decrease in the *c*-axis lattice parameter of the hexagonal graphite from $c = 6.721$ to 6.709 Å. Thus, the obvious conclusion is that sulfur is bonded only to the edges of graphite. Another puzzling result was obtained very recently by Campos-Delgado et al.[31] They synthesized graphene nanoribbons in large quantities (grams per day) by employing an aerosol pyrolysis process that used ferrocene, thiophene, and ethanol. The investigators were very surprised when they found that sulfur was not present in the graphene nanoribbons synthesized. The samples were composed of 85% of carbon and 15% of oxygen.

The experimental results obtained for graphite−sulfur composites and for the bulk production of graphene nanoribbons are very difficult to understand. On the one hand, sulfur is incorporated into graphite without problems, even at a 23 wt %. However, graphene nanoribbons do not present any amount of sulfur. To shed light into these experimental results and to investigate the properties of a graphene sheet functionalized with sulfur-containing groups, we have performed periodic first-principles calculations on perfect and defective graphene sheets functionalized with thioepoxide and thiol groups. In addition, we have used graphene nanoribbons to simulate the reactivities of the edges of graphene. This work continues our investigations about the interaction between sulfur and CNTs[29,30] and graphene sheets.[32] We expect that the results obtained can stimulate new

† E-mail: pablod@fq.edu.uy.

10.1021/jp808599w CCC: $40.75
Published on Web 03/18/2009

experimental investigations that pursue the synthesis of novel graphene−sulfur nanostructures.

2. Methods Section

The methodology employed is the same as that which we successfully used to study thioepoxidated[29] and thiolated[30] SWCNTs, sulfur-doped graphene,[32] and magnetic graphite.[33] Briefly, we have performed periodic density functional calculations employing the GGA (PBE parametrization)[34] and LDA functionals,[35] as implemented in the Siesta Program,[36,37] which performs SCF calculations using numerical basis sets. The interaction between ionic cores and valence electrons was described by the Troullier−Martins norm conserving pseudopotentials.[38] We have checked the convergence of the mesh cut off, and by employing a value of 200 Ry, we obtained converged binding energies. The basis set selected was the double-ζ basis set plus polarization functions (DZP), and the orbital confining cutoff was fixed to 0.01 Ry, following the recommendations of Rurali et al.[39] The graphene cells were sampled by employing a 30 × 30 × 2 Monkhorst_Pack sampling of around 1000 *k* points, similar to that employed by us to study sulfur-doped graphene[32] and magnetic graphite.[33] The DFT implementation in Siesta makes the results prone to big basis set superposition error (BSSE); therefore, we used the counterpoise correction suggested by Boys and Bernardi in 1970.[40] In all cases, we used relaxed structures to estimate the BSSE-corrected binding energies, and we took into account monomer deformation energies. The geometry optimizations were performed using the conjugate gradient algorithm until all residual forces were smaller than 0.01 eV/Å. Finally, we would like to note that in the previous works,[29,30,32,33] we have performed calibration of the methodology employed. The comparison showed that the methodology used is able to reproduce the results obtained without the use of pseudopotentials. Additional information about this comparison is presented in the Supporting Information.

To simulate perfect graphene sheets, we used a 4 × 4 × 1 and 5 × 5 × 1 supercells models; the number of atoms in each supercell was 32 and 50, respectively. Supercells of similar size have been successfully employed by us[32,33] and other investigators to study graphene sheets.[41−43] Single vacancy defects were created in the 4 × 4 × 1 and 5 × 5 × 1 supercells, removing a carbon atom. The properties obtained for the perfect and defective supercells were nearly the same for the 4 × 4 × 1 and 5 × 5 × 1 models.

Graphene nanoribbons were used to simulate the reactivity of the edges of graphene. The edges considered are the zigzag and armchair. On the one hand, we did not include any atoms to saturate the edges because a recent landmark work showed that graphene sheets can be produced in the gas phase with no hydrogen or oxygen atoms present.[44] Indeed, the average H content of these sheets is undetectable. The unit cells have 32 atoms for the zigzag model and 50 atoms for the armchair model. On the other hand, we used graphene nanoribbons with edges saturated with hydrogen atoms because it is a more real situation; a bare edge is extremely reactive. For the latter case, we have used a zigzag nanoribbon composed of 32 carbon atoms saturated with 8 hydrogen atoms per unit cell. The ribbons were sampled employing a 100 × 2 × 2 Monkhorst_Pack sampling.

Finally, since the entropy loss is expected to be significant, we have performed cluster model calculations to estimate free-energy changes. For that purpose, we used the B3LYP[45,46] method in conjunction with the 6-31G* basis set.[47] The model

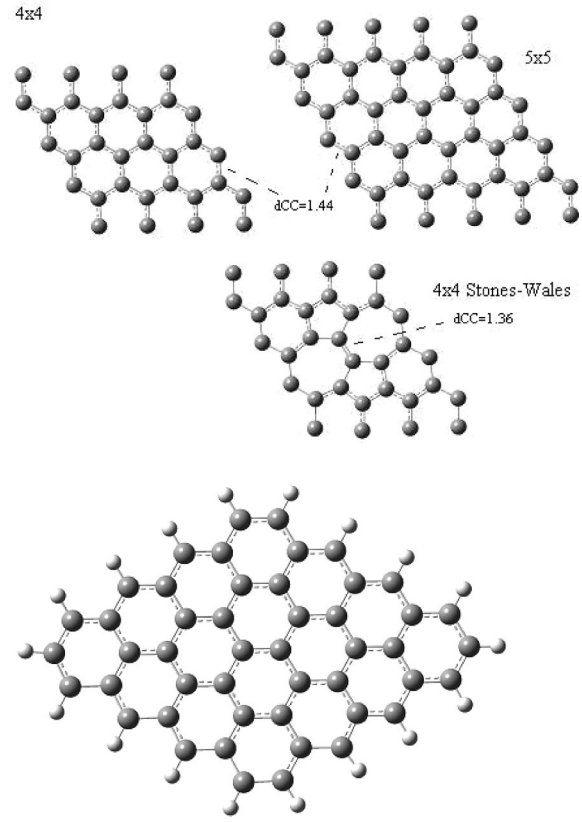

Figure 1. Optimized unit cells for the 4 × 4 and 5 × 5 graphene models, for the 4 × 4 model with a Stones−Wales defect and the $C_{48}H_{18}$ model employed in the cluster calculations. Distances in Å.

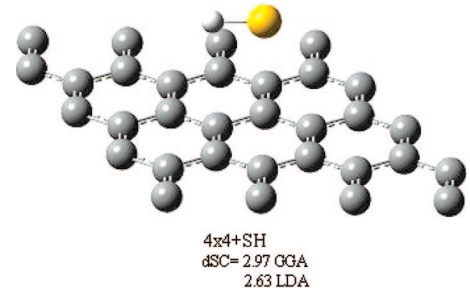

Figure 2. Optimized unit cell for the complex formed between the 4 × 4 graphene sheet and the SH group. Distances in Å.

employed to simulate graphene has the chemical formula $C_{48}H_{18}$ and is presented in Figure 1. It was constructed adding 12 benzene rings to a pyrene molecule. To investigate the addition of the thiol group, two SH molecules were attached to the central CC bond of the $C_{48}H_{18}$ model. In the case of the thioepoxide group, a sulfur atom was attached to the central CC bond of the $C_{48}H_{18}$ model; singlet and triplet states were investigated for the latter addition. The former was found to be more stable. In all cases, the structures were confirmed to be a minimum in the potential energy surface performing vibrational frequency analysis. Free energies were estimated at 298 K and 1 atm. The B3LYP calculations were performed employing Gaussian 03.[48]

3. Results and Discussion

3.1. Thiolation of Perfect Graphene. In Figure 1, we present the structure determined for the pristine graphene sheets, and in Figure 2, the structure of the complex formed with the SH group is shown. At the GGA level, we have found that the SH group is not chemically bound to the perfect sheet. Indeed, it is

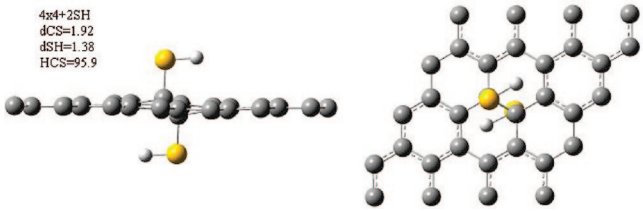

Figure 3. Optimized unit cell for the 4 × 4 graphene sheet interacting with two thiol groups SH. Distances in Å.

located 2.97 Å above it, and the interaction energy is null. While GGA can help us to decide whether or not a single thiol group can form a chemical bond with the sheet, it is incapable of predicting physisorption energies. For that reason, we have performed LDA calculations. Due to a fortuitous error cancelation, in some cases, LDA can give qualitative physisorption energies. Indeed, in a recent work,[49] we have shown that it can accurately reproduce the interaction between methane and SWCNTs. At the LDA level, the SH group is 2.63 Å above the sheet, and the system is bound by 0.28 eV, very large for a van der Walls energy but expected because of the radical character of the SH group. Overall, the GGA and LDA results suggest that the interaction between a single SH group and perfect graphene is small.

In a previous work,[30] we have observed that the binding energy between a single SH group and a perfect (5,5) SWCNT is small. However, it is increased from 0.35 to 0.51 eV if two SH groups are attached to the same CC bond. For that reason, we have investigated this possibility for graphene. Six arrangements were considered for two SH groups, (a) two SH groups in the ortho position on the same side of the sheet, (b) two SH groups in meta positions on the same side of the sheet, (c) two SH groups in para positions on the same side of the sheet, (d) the same as that in (a) but with the SH groups on opposite sides of the sheet, as indicated in Figure 3, (e) the same as that in (b) but on opposite sides of the sheet, and (f) the same as that in (c) but on opposite sides of the sheet. At the GGA level, in the cases (a), (b), (c), (d), and (e), we have found that the interaction energy is very small or that HSSH is formed (case a). However, in case (d), that presented in Figure 3, the system is chemically bound, and the binding energy per SH group is 0.36 eV. This behavior is similar to that observed for the hydrogenated SWCNTs, which prefer the attachment on H atoms inside and outside of the tube.[50] Moreover, this finding is also in agreement with the observations made in a landmark investigation by Galano[51] for the attachment of radicals to SWCNTs; once a radical is attached, further additions are increasingly feasible. Since two SH groups have a much more larger binding energy than a single thiol group, we have considered the addition of four SH groups in alternating and consecutive positions, as indicated in Figure 4. We expected a much larger binding energy than that determined for two SH groups, but this was not the case. The binding energy per SH group was very similar to the previous case, 0.38 eV. Thus, it seems unlikely that the binding energy per SH group will reach a value large enough to consider that the thiol groups are strongly bonded to perfect graphene.

3.2. Thiolation of Defective Graphene. The first defect considered is the Stones−Wales (SW) one.[52−54] In Figure 1, we present the structure of the 4 × 4 supercell containing the SW defect. For the 4 × 4 supercell, we have found that the formation energy of the latter defect is 4.1 eV, in good agreement with the formation energy equal to 3.7 eV, reported by Zurek et al.[52] for a SW defect in a (10,0) SWCNT. However, our result is 1.1 eV larger than that reported by Ouyang et al.[54]

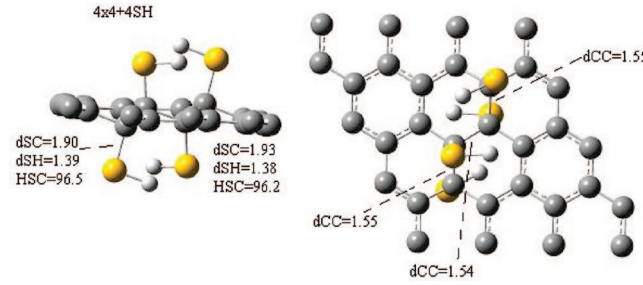

Figure 4. Optimized unit cell for the 4 × 4 graphene sheet interacting with four thiol groups SH. Distances in Å.

TABLE 1: Bindingd Energies Determined between Graphene and the SH, S, OH, and O Groups in Different Configurations

	number of SH groups	position	binding energy (eV)
$G44_{perfect}$	1	C	0.28[a]
$G44_{Stones-Wales}$	1	C_{757}	0.46[b]
$G44_{Stones-Wales}$	1	C_{765}	0.18[b]
$G44_{perfect}$	2	para, same side[d]	0.10
$G44_{perfect}$	2	ortho, opp. side	0.36[b]
$G44_{perfect}$	2	para, opp. side[e]	0.06
$G44_{Stones-Wales}$	2	CC bond opp. side	1.10[b]
$G44_{perfect}$	4	chain, alternating sides	0.38[b]
zigzag ribbon	1	H-saturated edge	1.6[b]
$C_{48}H_{18}$	2	ortho, opp. side	0.25[c]

	group	position	einding Energy (eV)
$G44_{perfect}$	S	CC bond	0.48[b]
$C_{48}H_{18}$	S	CC bond	0.1[c]
$G44_{perfect}$	O	CC bond	1.80[b]
$G44_{perfect}$	OH	C atom	0.53[b]

[a] Determined at the LDA level using infinite models. LDA was used because the SH groups is physisorbed. [b] Determined at the GGA level using infinite models. [c] Determined at the B3LYP/6-31G* level. [d] The meta and ortho isomers prefer to detach SH and form HSSH. [e] The meta isomer migrated to the ortho isomer upon optimization.

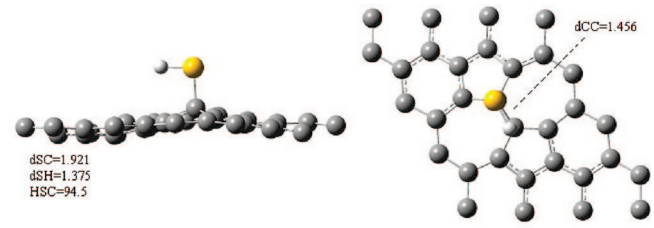

Figure 5. Optimized unit cell for the 4 × 4 graphene model containing a Stones−Wales defect and a single SH group attached. Distances in Å.

for a graphene nanoribbon. We have investigated two additions; (a) we attached a SH group to a carbon atom of the shortest CC bond, that which connects the pentagons, and (b) we attached the SH group to a carbon atom that is shared by a pentagon, hexagon, and heptagon. The binding energies determined are 0.46 and 0.18 eV for cases (a) and (b), respectively (see Table 1). Figure 5 shows the structure and most important bond distances for the adduct formed between the defective sheet and the SH group. The binding energy determined for case (a) is much larger than that determined for a perfect sheet, but it is too small in terms of a chemical bonding picture. However, if a second SH group is attached to the same CC bond but on the opposite side of the sheet (similar to Figure 3 but on the SW defect), the binding energy is increased to 1.1 eV per SH group.

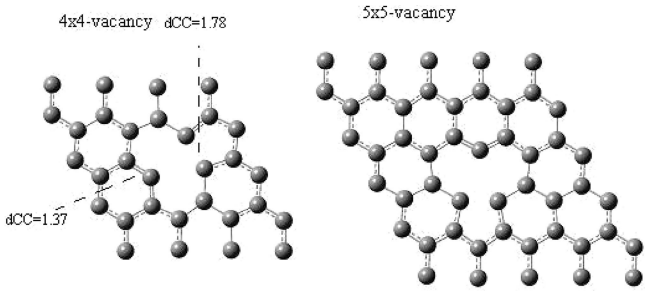

Figure 6. Optimized unit cell for the 4 × 4 and 5 × 5 graphene models containing a single vacancy defect. Distances in Å.

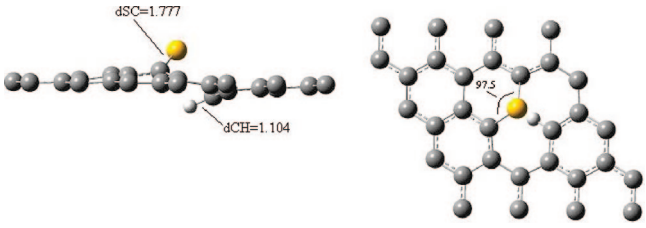

Figure 7. Optimized unit cell for the 4 × 4 graphene model containing a single vacancy defect and the SH group dissociatively added, side view (left) and top view (right). This structure is 2.6 eV more stable than that which has the SH group attached to the vacancy. Distances in Å; angles in degrees.

The second defect considered is the single vacancy defect site. In Figure 6, we report the structure of the defective supercell optimized. In agreement with our previous work about defective magnetic graphite,[33] we found that the system has a permanent magnetic moment, 1.2 and 1.4 μ_B for the 4 × 4 and 5 × 5, models, respectively. This result is in good agreement with that reported by Ma et al.,[55] 1.04 μ_B for a graphene model composed of 128 carbon atoms. The formation energy of the vacancy defect site is 7.50 eV for the 4 × 4 sheet and 7.53 eV for the 5 × 5 sheet, in excellent agreement with the experimental value of 7 ± 0.5 eV.[56] The results obtained for the 4 × 4 and 5 × 5 models indicate that the extension of the size of the supercell will not introduce important changes into the values reported herein. Indeed, Ma et al.[55] determined for a graphene model containing 128 atoms that the formation energy of the vacancy defect site is 7.7 eV, very close to our prediction. It is important to note that Ma et al.[55] employed plane wave methodologies. Therefore, the latter comparison can be considered as a benchmark between the very accurate plane wave methodologies and the LCOA approach. Finally, as observed by Ma et al.,[55] we appreciate a small Jahn−Teller distortion of the sheet; the C atom that has a dangling bond is lifted a bit from the plane of the sheet, namely, 0.08 Å.

Several additions were considered between the defective sheet and the SH group. Figure 7 shows the most stable one; the SH group is dissociatively attached to the vacancy defect site. The sulfur atom reconstructs a hexagon, and the hydrogen atom is attached to the carbon atom that has a dangling bond. The new hybrid formed between the sheet and the S and H atoms has a permanent magnetic moment of 1 μ_B. We have considered the attachment of the undissociated SH group to the vacancy defect site, but the structure is much less stable than that previously discussed by 2.6 eV. Other additions were considered, such as the formation of S-doped graphene[32] with an H atom attached to a carbon atom. However, all of them were found to be higher in energy than that presented in Figure 7; they are presented in the Supporting Information.

3.3. Thiolation at the Edges. It is well-known that bare edges are extremely reactive, although they are present in large quantities in graphene nanoribbons synthesized in the gas phase.[44] We have simulated the reactivity of the bare zigzag and armchair edges, employing bare graphene nanoribbons. In both cases, we have observed that when the SH group is attached to the edge, the closest carbon atom subtracts the hydrogen atoms from sulfur, and a CH bond is formed. As expected, the process is extremely exothermic, close to 6.5 eV. Finally, we have simulated the reactivity of a zigzag edge saturated with H atoms. To that end, we used a zigzag graphene nanoribbon composed of 32 carbon atoms and 8 H atoms per unit cell. The results indicated that, despite the presence hydrogen atoms, the edge is reactive against the SH group and the C−SH binding energy is 1.6 eV. The dissociative attachment of the SH radical at the edge was investigated, but it was found to be slightly less favorable than the previous case by 0.3 eV. The present results show that the single vacancy defect site and the zigzag edges of graphene present the same chemical behavior, being the most reactive sites of the sheet.

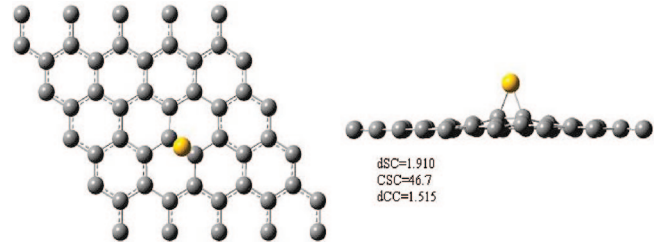

Figure 8. Optimized unit cell for the 5 × 5 graphene model containing a single S atom. Distances in Å.

3.4. Thioepoxidated Graphene. It has been demonstrated that graphite[14] and graphene[13] oxide present a large number of epoxide groups; because sulfur belongs to the same group as oxygen, it is interesting to study if the sulfur atom can form a thioepoxide group on graphene. We present the structure of the thioepoxidated graphene in Figure 8. We have found that a single sulfur atom can be attached to graphene, although the binding energy is small, 0.48 and 0.49 eV for the 4 × 4 and 5 × 5 graphene models, respectively. As expected, considering the small binding energy, the CS distance is 1.910 Å, much longer than that observed in a typical single CS bond. This result is in good agreement with our previous findings which suggested a binding energy of 1.44 eV for the attachment of a single sulfur atom to a (10,0) SWCNT (parallel to the tube axis). Thus, we can confirm an important decrease of the reactivity of the SWCNTs against the sulfur atom when the diameter is increased because of their lower curvature.

3.5. Importance of Free Energy. In recent investigations by Galano[51] and Okamoto,[57] it was shown that it is very important to include free-energy corrections to understand the attachment of radicals on SWCNTs[51] and the adsorption of H_2 by the $Ti_2-C_2H_4$ complex. To gauge the spontaneity of the adsorption of SH and S on graphene, cluster model calculations were performed, as described in section 2. The structure of the adduct formed by the $C_{48}H_{18}$ model and the thiol groups is presented in Supporting Information Figure 5.S1. The adsorption energy of two SH groups to the same CC bond and on opposite sides of the $C_{48}H_{18}$ model is 0.25 eV/SH at the B3LYP/6-31G* level of theory. This value is only 0.1 eV lower than that determined by employing the PBE functional and periodic boundary conditions. Therefore, the cluster model calculations confirm that perfect graphene has a very low reactivity against the SH group. Indeed, when enthalpy and free-energy corrections are included, the reaction becomes less favorable; the enthalpy change is −0.10 eV, and the free-energy change is positive by

0.81 eV, confirming the previous statement; the process is very unlikely to occur, mostly due to the significant entropy loss.

The structure of the adduct formed by the $C_{48}H_{18}$ and the S atom is presented in Supporting Information Figure 6.S1. At the B3LYP/6-31G* level, the binding energy is only 0.10 eV, about 0.4 eV smaller than that determined employing Siesta. As observed for the thiolation, the inclusion of the free-energy correction (0.42 eV) shows that the process is not favorable ($\Delta G > 0$), 0.32 eV. Therefore, if this correction is included to our infinite model, the process will have $\Delta G \approx 0$, and the addition will be very unlikely to occur. We want to note that this is a very approximate estimation of the free-energy corrections for surfaces, but in qualitative terms, the corrections calculated can help us understand whether or not they are possible.

3.6. Electronic Properties. Graphene is a zero band gap semiconductor; in Figure 9, we show the total density of states determined for the perfect sheet. The introduction of defects such as the Stones−Wales and the vacancy defect sites induce important changes in the density of states. They are reported in Figure 9. In the case of the Stones−Wales defect, the Fermi level moves 0.1 eV toward higher energies, and the strong peak observed 1.7 eV above the Fermi level moves toward lower energies and now is located 0.37 eV above the Fermi level. The DOS determined for the graphene sheet containing a single vacancy indicates that the graphene sheet is a metal. The Fermi level moves to lower energies, about 0.51 eV lower than that in the perfect sheet.

For perfect graphene, we have found that the thiolation can have very different effects. In the case of two SH groups added to the same CC bond, the DOS presented in Figure 10 indicates that the sheet is metallic. However, when the number of SH groups is increased to four, the sheet is a small band gap semiconductor (0.15 eV). These results are in good agreement with those obtained for thiolated SWCNTs[30] and for sulfur-doped graphene.[32] In the latter works, we have found that the electronic properties of the hybrids depend on the structural changes induced on the sheet by the number and position of functional groups added/substituted. Indeed, the S-doped sheet can be a small gap semiconductor or have better metallic properties than that of the pristine sheet depending on the number of S atoms included.[32] In the case of the sheet containing a Stones−Wales defect, we have found that the thiolation at the CC bond which connects the two pentagons gives some metallic character to the sheet. The DOS obtained is very similar to that presented for the graphene sheet containing a single vacancy. In Figure 11 are plots of the DOS of the graphene sheet containing a single vacancy defect site and the SH group dissociatively attached to the defect, as indicated in Figure 7. The DOS at the Fermi level is strongly modified upon H and S chemisorption. For the high spin, the DOS is zero, just above the Fermi level, whereas that of the low spin is zero below the Fermi level.

When graphene has a single sulfur atom attached, the electronic properties are very similar to those observed for the pristine sheet, as we can appreciate in Figure 12. The DOS at the Fermi level is slightly increased, but the pseudogap still exists. We expect that, as observed for the sulfur-doped graphene,[32] the multiple addition of thioepoxide groups can tune the electronic properties of the sheet.

3.7. Implications for Experiment. It is well-known that perfect graphene is less reactive than carbon nanotubes. Indeed, quite recently, Wang et al.[58] could not deposit metal oxides on graphene sheets because they were unreactive. The different

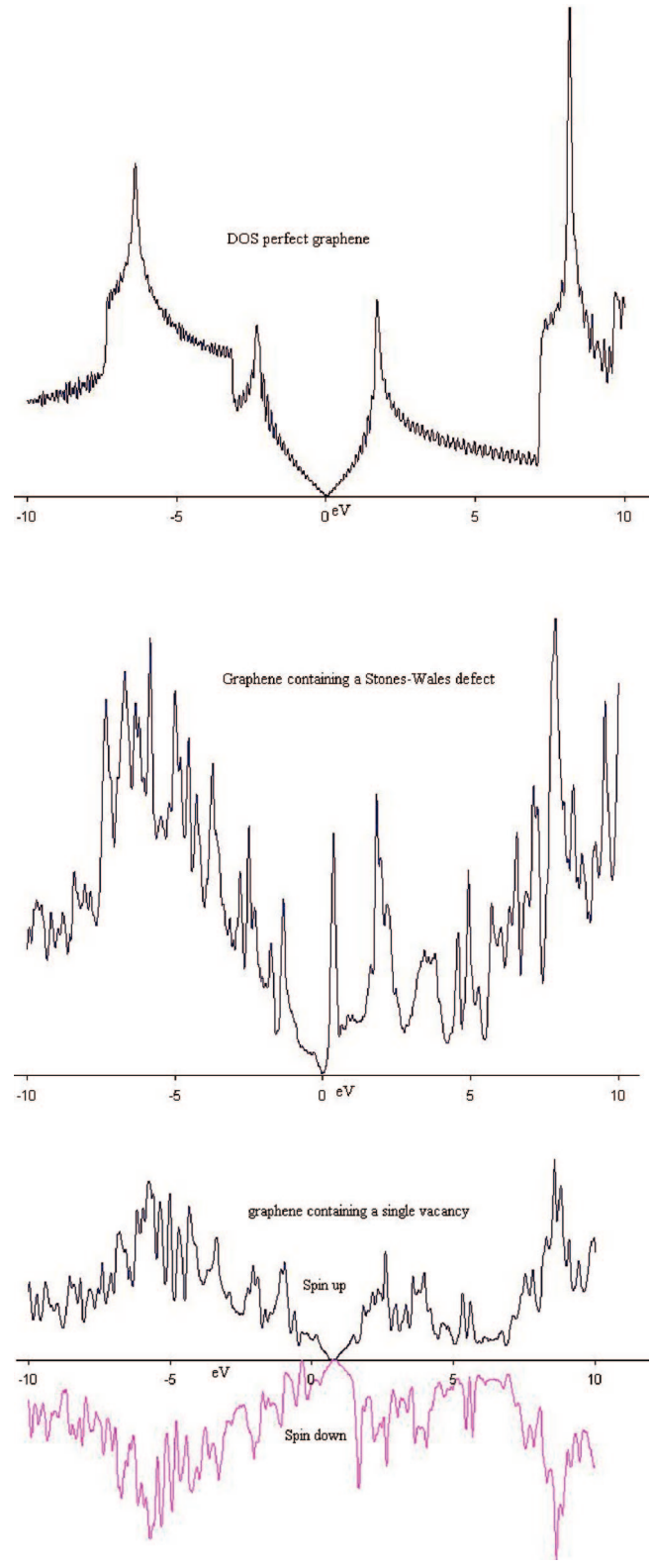

Figure 9. Density of states determined for the perfect graphene sheet (top), Stones−Wales defective sheet (middle), and the sheet containing a single vacancy defect site (bottom).

reactivities observed for the perfect sheet, defect sites, and edges suggest that the SH group can be used to label the defect present in graphene sheets. In addition, these thiol groups can be used to attach gold nanoparticles or to anchor the graphene sheet on a Au(111) surface.[59−61] Indeed, Maksymovych et al.[61] found that even an undissociated CH_3SH molecule binds to an atop Au(111) site on a defect-free Au(111) surface. The binding

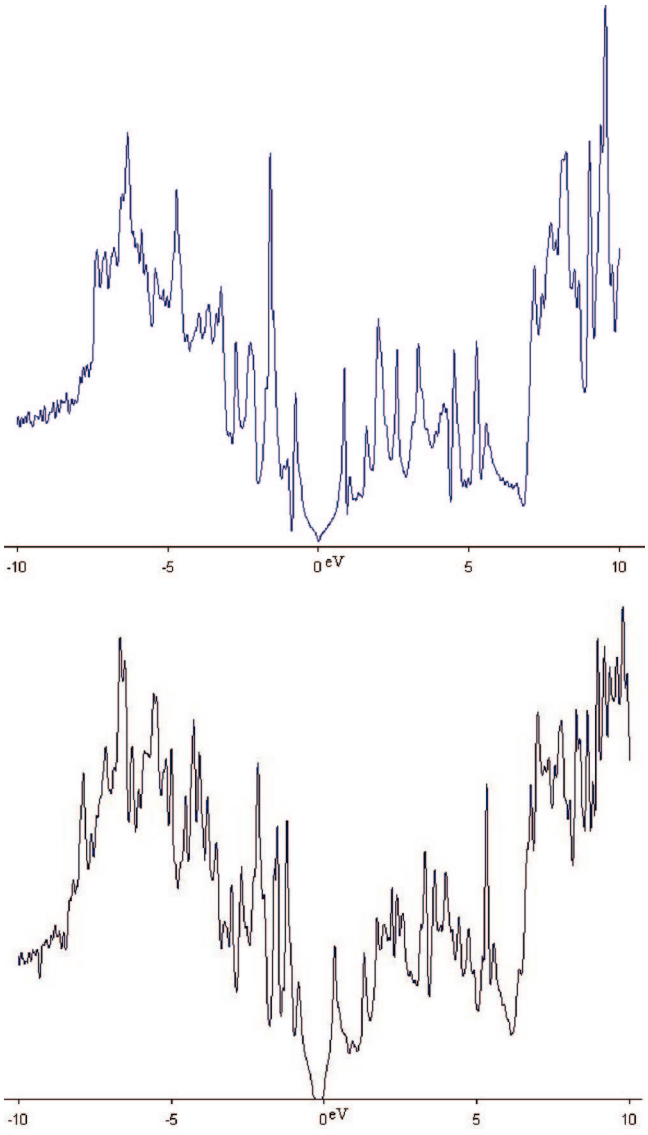

Figure 10. Density of states determined for the perfect graphene sheet functionalized with two SH groups (top) and with four SH groups (bottom).

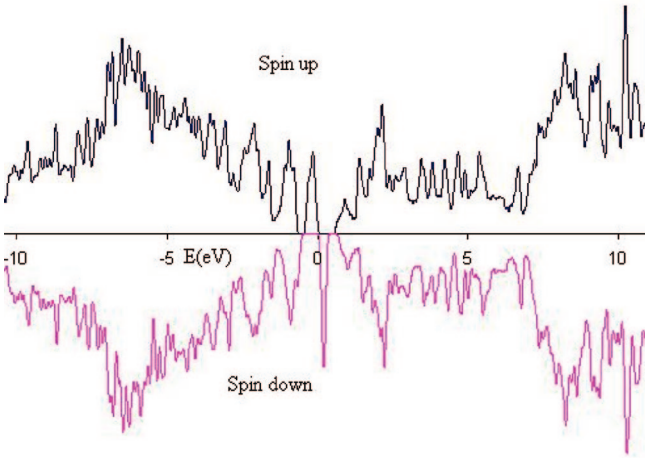

Figure 11. Density of states determined for the 4 × 4 graphene model containing a single vacancy defect site and the SH group dissociatively added (Figure 7).

energy between the gold surface and CH_3SH is 8.6 kcal/mol. Since the edges and defects can attach several SH groups, we

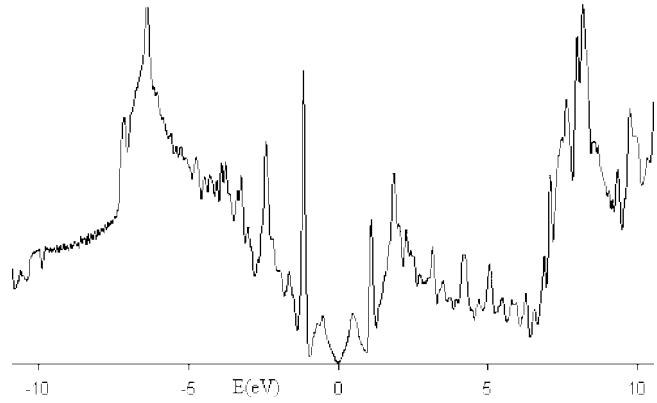

Figure 12. Density of states determined for the perfect graphene (G55 model, 50 atoms) sheet functionalized with a single sulfur atom (Figure 8).

can have an huge binding energy between the sheet and gold nanoparticles or gold surfaces. For example, a sheet containing 30 SH groups on the edge will have a binding energy of 240 kcal/mol with a perfect Au surface, and this energy can be increased if the surface has defects or the SH groups are dissociatively attached to the edges. Thus, it will be very easy to create vertically aligned graphene sheets on gold surfaces if SH groups are employed because of the selective binding properties that they have.

3.8. Comparison with Graphite Oxide. The attachment of oxygen atoms and hydroxyl groups to graphene and graphite has been extensively studied[63−68] because graphite oxide is one of the precursors of graphene sheets since it can be reduced by employing hydrazine. It has been shown[63−68] that the oxygen atom can bind graphene to form an epoxide-like structure. The values suggested for the binding energy between the O atom and the sheet are 1.9,[63] 2.5,[65] and 1.1 eV.[67] The former value was determined at the PW91 level by employing plane wave methodologies, the second value was estimated by employing the same methodology but a smaller unit cell, and the last one was calculated by employing the B3LYP functional and a $C_{42}H_{16}$ cluster model. The value determined by us, using the same methodology as that for the S and SH groups, is 1.8 eV, in excellent agreement with that suggested by Sorescu et al.[63] We believe that the latter value is the most accurate one because the authors employed periodic conditions and the largest supercells among the works cited. Thus, this comparison constitutes another proof of the accuracy of the procedure selected by us.

The binding determined for the oxygen atom is 4 times larger than that calculated for sulfur, something that can be understood by considering that the electron-withdrawing capabilities of sulfur are smaller than those of the oxygen atom, and thus, the C−S bond is weaker. The C−O bond distance is 1.465 Å, much closer to a typical C−O single bond than that in the case of the C−S one (1.911 Å). For the OH group, we have determined that the binding energy with graphene is 0.53 eV, nearly the same value as that determined in ref 65. This value seems to be quite small to attach a single OH group to perfect graphene. Indeed, as observed for the thiol group, we expect that $\Delta G \approx 0$. Therefore, the present results indicate that the OH groups attached to graphene should be present at defect sites, or they must be agglomerated to increase the binding energy due to cooperative binding. This observation is supported by solid-state 13C NMR spectra of graphite oxide.[68] Indeed, He et al.[68] showed that graphite oxide is composed of aromatic islands that

are separated from each other by aliphatic rings containing OH and epoxide groups. The latter results show that the OH group cannot be attached to perfect graphene. The SH group can be physisorbed on perfect graphene but not chemisorbed. Thus, in contrast with the case of graphene oxide, the attachment of S and SH groups to graphene can be possible only if defects and edges are present, allowing the chemical labeling of these sites.

4. Conclusions

The thiolation and thioepoxidation of perfect and defective graphene have been investigated by employing first-principles calculations. The following are the most important conclusions of the present work.

(1) Perfect graphene has a very low reactivity against the thiol group. Multiple additions to the sheet can increase the binding energy, but the bonding is still too weak. The free-energy change for this process is expected to be unfavorable.

(2) Graphene sheets containing a Stones−Wales defects are more reactive than pristine sheets, although to observe a large binding energy the groups must be attached to the same CC bond and on opposite sides of the sheet. For the latter configuration, the binding energy is 1.1 eV per SH group. In the case of cooperative addition on the SW defect, the expected free-energy change is expected to be favorable, but that of a single SH group is not.

(3) The single vacancy defect site is extremely reactive against the SH group, and it has the same chemical behavior as a bare edge since it favors the dissociative attachment of a SH group. The system has a permanent magnetic moment of 1 μ_B.

(4) The bare edges are extremely reactive against the thiol group. Indeed, it is dissociatively bonded to the edge. The process is favorable by 6−7 eV for the zigzag and armchair unsaturated edges. The zigzag edge saturated with a hydrogen atom is reactive against a single SH, and the system has a magnetic moment. The binding for a single SH group is 1.6 eV.

(5) The different reactivities observed for the perfect sheet, defect sites, and edges indicate that thiolation can be used as an effective method to label defects and zigzag edges in graphene sheets, carbon nanoribbons, and nanotubes. Thus, the SH groups can be used to create vertically aligned graphene sheets on gold surfaces or to selectively attach/detach biological molecules.[28]

(6) The attachment of a sulfur atom to perfect graphene has a small binding, 0.49 eV, and the free-energy change is expected to be very close to 0. Thus, it is unlikely that it can be achieved experimentally.

(7) The small reactivity of the perfect graphene sheet against thiolation and thioepoxidation suggests that very large diameter perfect SWCNTs will have a small binding energy with the S[29] and SH[30] groups. This supports our previous findings[29,30] which indicated that only small diameter SWCNTs, HiPco ones, for example,[62] and defective tubes will react with the above-mentioned groups.

(8) The reactivities observed for S and SH confirm previous experimental[26,27] investigations, which suggested that in superconductive sulfur−graphite composites, the sulfur atoms are present only at the edges of the tubes, although defect sites must be considered to understand the effect because they can easily attach sulfur-containing groups. However, it is difficult to understand why Campos-Delgado et al.[31] did not observe sulfur in the bulk production of graphene nanoribons. The most reasonable explanation is that the ribbons prefer to bind oxygen rather than sulfur, something reasonable considering the binding energies determined. Perhaps sulfur can be attached to the ribbons if the source of sulfur is changed to the bulk form and the amount is increased.

(9) The binding energy between a single OH group and graphene is small, 0.5 eV. As observed for the thiol group, we expect that $\Delta G \approx 0$. Therefore, the present results indicate that it is due to the free-energy correction that the OH groups graphene oxide are present at defect sites and agglomerated to increase the binding energy due to cooperative binding. These results confirm the earlier solid-state NMR results obtained by He et al.[68] which detected the presence of aromatic islands separated from aliphatic rings containing OH and epoxide groups.

Acknowledgment. The author thanks the PEDECIBA Quimica and CSIC for financial support. The author wants to express his gratitude to the reviewers for useful comments that contributed to improve the manuscript.

Supporting Information Available: Additional structure and energy results. This material is available free of charge via the Internet at http://pubs.acs.org.

References and Notes

(1) Iijima, S. *Nature* **1991**, *354*, 56.
(2) Lim, S.; Li, N.; Fang, F.; Pinault, M.; Zoican, C.; Wang, C.; Fadel, T.; Pfefferle, L. D.; Haller, G. L. *J. Phys. Chem. C* **2008**, *112*, 12442.
(3) Li, X.; Tu, X.; Zaric, S.; Welsher, K.; Seo, W. S.; Zhao, W.; Dai, H. *J. Am. Chem. Soc.* **2007**, *129*, 15770.
(4) Li, Q.; Ren, W.; Chen, Z.-C.; Wand, D.-W.; Liu, B.; Yu, B.; Li, F.; Cong, H.; Chen, H.-M. *ACS Nano* **2008**, *2*, 1722.
(5) Mawhinney, D. B.; Naumenko, V.; Kuznetsova, A.; Yates, J. T.; Liu, J.; Smalley, R. E. *Chem. Phys. Lett.* **2000**, *324*, 213.
(6) Bao, Q.; Zhang, J.; Pan, C.; Li, J.; Li, C. M.; Zang, J.; Tang, T. Y. *J. Phys. Chem. C* **2007**, *111*, 10347.
(7) Okada, S. *Chem. Phys. Lett.* **2007**, *447*, 263.
(8) Amorim, R. G.; Fazzio, A.; Antonelli, A.; Novaes, F. D.; da Silva, A. J. R. *Nano Lett.* **2007**, *7*, 2459.
(9) Braga, S. F.; Coluci, V. R.; Baughman, R. H.; Galvao, D. S. *Chem. Phys. Lett.* **2007**, *441*, 78.
(10) Ding, F.; Lin, Y.; Krasnov, P. O.; Yakobson, B. I. *J. Chem. Phys.* **2007**, *127*, 164703.
(11) Novoselov, K. S.; Geim, A. K.; Morozov, S. V.; Jiang, D.; Zhang, Y.; Dubonos, S. V.; Grigorieva, I. V.; Firson, A. A. *Science* **2004**, *306*, 666.
(12) Novoselov, K. S.; Geim, A. K.; Morozov, S. V.; Jiang, D.; Katsnelson, M. I.; Grigorieva, I. V.; Dubonos, S. V.; Firsov, A. A. *Nature* **2005**, 438–197.
(13) Li, J.-L.; Kudin, K. N.; McAllister, M. J.; Prud'homme, R. K.; Aksay, I. A.; Car, R. *Phys. Rev. Lett.* **2006**, *96*, 176101.
(14) Paci, J. T.; Belytschko, T.; Schatz, G. C. *J. Phys. Chem. C* **2007**, *111*, 18099.
(15) Lee, C.; Wei, X.; Kysar, J. W.; Hone, J. *Science* **2008**, *321*, 385.
(16) Gomez-Navarro, C.; Burghard, M.; Kern, K. *Nano Lett.* **2008**, *8*, 2045.
(17) Balandin, A. A.; Suchismita, G.; Bao, W.; Calizo, I.; Teweldebrhan, D.; Miao, F.; Lau, C. N. *Nano Lett.* **2008**, *8*, 902.
(18) Au, A.; Ramesh, P.; Itkis, M. E.; Bekyarova, E.; Haddon, R. C. *J. Phys. Chem. C* **2007**, *111*, 7565.
(19) Williams, G.; Seger, B.; Kamat, P. V. *ACS Nano* **2008**, *7*, 1487.
(20) Deifallah, M.; McMillan, P. F.; Cora, F. *J. Phys. Chem. C* **2008**, *112*, 5447.
(21) Lu, H.; He, P. M.; Feng, Y. P. *J.Phys. Chem. C* **2008**, *112*, 12683.
(22) Liu, Z.; Robinson, J. T.; Sun, X.; Dai, H. *J. Am. Chem. Soc.* **2008**, *130*, 10876.
(23) Muszynski, R.; Seger, B.; Kamat, P. V. *J. Phys. Chem. C* **2008**, *112*, 5263.
(24) Ao, Z. M.; Yang, J.; Li, S.; Jiang, Q. *Chem. Phys. Lett.* **2008**, *461*, 276.
(25) Wehling, T. O.; Novoselov, K. S.; Morozov, S. V.; Vdovin, E. E.; Katsnelson, M. I.; Geim, A. K.; Lichtenstein, A. I. *Nano Lett.* **2008**, *8*, 173.
(26) Kurmaev, E. Z.; Galakhov, A. V.; Moewes, A.; Moehlecke, S.; Kopelevich, Y. *Phys. Rev. B* **2002**, *66*, 193402.
(27) Da Silva, R. R.; Torres, J. H. S.; Kopelevich, Y. *Phys. Rev. Lett.* **2001**, *87*, 147000.

(28) You, Y.-Z.; Hong, C.-Y.; Pan, C.-Y. *J. Phys. Chem. C* **2007**, *111*, 16161.
(29) Denis, P. A.; Faccio, R. *Chem. Phys. Lett.* **2008**, *460*, 486.
(30) Denis, P. A. *Int. J. Quantum Chem.* **2009**, *109*, 772.
(31) Campos-Delgado, J.; Romo-Herrera, J. M.; Jia, X.; Cullen, D. A.; Muramatsu, H.; Kim, Y. A.; Hayashi, T.; Ren, Z.; Smith, D. J.; Okuno, Y.; Ohba, T.; Kanoh, H.; Kaneko, K.; Endo, M.; Terrones, H.; Dresselhaus, M. S.; Terrones, M. *Nano Lett.* **2008**, *8*, 2773.
(32) Denis, P. A.; Faccio, R.; Mombru, A. W. *ChemPhysChem* **2009**, *10*, 715.
(33) Faccio, R.; Pardo, H.; Denis, P. A.; Oreiras, Y.; Araujo-Moreira, F. M.; Verisimo-Alves, M.; Mombru, A. W. *Phys. Rev. B.* **2008**, *77*, 035416.
(34) Perdew, J. P.; Burke, K.; Ernzerhof, M. *Phys. Rev. Lett.* **1996**, *77*, 3865.
(35) Perdew, J. P.; Zunger, A. *Phys. Rev. B* **1981**, *23*, 5048.
(36) Soler, J. M.; Artacho, E.; Gale, J. D.; Garcia, A.; Junquera, J.; Ordejon, P.; Sanchez-Portal, D. *J. Phys.: Condens. Matter* **2002**, *14*, 2745.
(37) Ordejon, P.; Artacho, E.; Soler, J. M. *Phys. Rev. B* **1996**, *53*, R10441.
(38) Troullier, N.; Martins, J. L. *Phys. Rev. B* **1991**, *43*, 1993.
(39) Rurali, R. N.; Lorente, N.; Ordejon, P. *Phys. Rev. Lett.* **2007**, *95*, 209601.
(40) Boys, F. S. F.; Bernardi, F. *Mol. Phys.* **1970**, *19*, 553.
(41) Cabrera-Sanfelix, P.; Darling, G. R. *J. Phys. Chem. C* **2007**, *111*, 18258.
(42) Zanella, I.; Fagan, S. B.; Mota, R.; Fazzio, A. *J. Phys. Chem. C* **2008**, *112*, 9163.
(43) Chan, K.; Neaton, J. B.; Cohen, M. L. *Phys. Rev. B* **2008**, *77*, 235430.
(44) Dato, A.; Radmilovic, V.; Lee, Z.; Philips, J.; Frenklach, M. *Nano Lett.* **2008**, *8*, 2012.
(45) Becke, A. D. *J. Chem. Phys.* **1993**, *98*, 5648.
(46) Lee, C.; Yang, W.; Parr, R. G. *Phys. Rev. B* **1988**, *37*, 785.
(47) Ditchfeld, R.; Hehre, W. J.; Pople, J. A. *J. Chem. Phys.* **1971**, *54*, 724.
(48) Frisch, M. J.; Trucks, G. W.; Schlegel, H. B.; Scuseria, G. E.; Robb, M. A.; Cheeseman, J. R.; Montgomery, J. A., Jr.; Vreven, T.; Kudin, K. N.; Burant, J. C.; Millam, J. M.; Iyengar, S. S.; Tomasi, J.; Barone, V.; Mennucci, B.; Cossi, M.; Scalmani, G.; Rega, N.; Petersson, G. A.; Nakatsuji, H.; Hada, M.; Ehara, M.; Toyota, K.; Fukuda, R.; Hasegawa, J.; Ishida, M.; Nakajima, T.; Honda, Y.; Kitao, O.; Nakai, H.; Klene, M.; Li, X.; Knox, J. E.; Hratchian, H. P.; Cross, J. B.; Bakken, V.; Adamo, C.; Jaramillo, J.; Gomperts, R.; Stratmann, R. E.; Yazyev, O.; Austin, A. J.; Cammi, R.; Pomelli, C.; Ochterski, J. W.; Ayala, P. Y.; Morokuma, K.; Voth, G. A.; Salvador, P.; Dannenberg, J. J.; Zakrzewski, V. G.; Dapprich, S.; Daniels, A. D.; Strain, M. C.; Farkas, O.; Malick, D. K.; Rabuck, A. D.; Raghavachari, K.; Foresman, J. B.; Ortiz, J. V.; Cui, Q.; Baboul, A. G.; Clifford, S.; Cioslowski, J.; Stefanov, B. B.; Liu, G.; Liashenko, A.; Piskorz, P.; Komaromi, I.; Martin, R. L.; Fox, D. J.; Keith, T.; Al-Laham, M. A.; Peng, C. Y.; Nanayakkara, A.; Challacombe, M.; Gill, P. M. W.; Johnson, B.; Chen, W.; Wong, M. W.; Gonzalez, C.; Pople, J. A. *Gaussian 03*, revision B.04; Gaussian, Inc.: Pittsburgh, PA, 2003.
(49) Denis, P. A. *Chem. Phys.* **2008**, *353*, 79.
(50) Bauschlicher, C. W.; So, C. R. *Nano Lett.* **2002**, *2*, 337.
(51) Galano, A. *J. Phys. Chem. C* **2008**, *112*, 8922.
(52) Zurek, E.; Pickard, C. J.; Autschbach, J. *J. Phys. Chem. C* **2008**, *112*, 11744.
(53) Stone, A. J.; Wales, D. J. *Chem. Phys. Lett.* **1986**, *128*, 501.
(54) Ouyang, F.; Huang, B.; Li, Z.; Xiao, J.; Wang, H.; Xu, H. *J. Phys. Chem. C* **2008**, *112*, 12003.
(55) Ma, Y.; Lehtinen, P. O.; Foster, A. O.; Nieminen, R. M. *New J. Phys.* **2004**, *6*, 68.
(56) Thrower, P. A.; Mayer, R. M. *Phys. Status Solidi A* **1978**, *47*, 11.
(57) Okamoto, Y. *J. Phys. Chem. C* **2008**, *112*, 17721.
(58) Wang, X.; Tabakman, S. M.; Dai, H. *J. Am. Chem. Soc.* **2008**, *130*, 8152.
(59) Ulman, A. *Chem. Rev.* **1996**, *96*, 1533.
(60) Wang, Y.; Hush, N. S.; Reimers, J. R. *J. Am. Chem. Soc.* **2007**, *129*, 14532.
(61) Maksymovych, P.; Sorescu, D. C.; Dougherty, D.; Yates, J. T. *J. Phys. Chem. B* **2005**, *109*, 22463.
(62) Nikolaev, P.; Bronikowski, M. J.; Bradley, R. K.; Rohmund, F.; Colbert, D. T.; Smith, K. A.; Smalley, R. E. *Chem. Phys. Lett.* **1999**, *313*, 91.
(63) Sorescu, D. C.; Jordan, K. D.; Avouris, P. *J. Phys. Chem. B* **2001**, *105*, 11227.
(64) Collington, B.; Hoang, P. N. M.; Picaud, S.; Rayez, J. C. *Chem. Phys. Lett.* **2005**, *406*, 430.
(65) Jelea, A.; Marinelli, F.; Ferro, Y.; Allouche, A.; Brosset, C. *Carbon* **2004**, *42*, 3189.
(66) Ferro, Y.; Allouche, A.; Marinelli, F.; Brosset, C. *Surf. Sci.* **2004**, *559*, 158.
(67) Incze, A.; Pasturel, A.; Chatillon, C. *Surf. Sci.* **2003**, *537*, 55.
(68) He, H.; Klinowski, J.; Forster, M.; Lerf, A. *Chem. Phys. Lett.* **1998**, *287*, 53.

JP808599W